

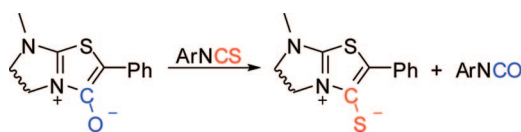
## Thionation of Mesoionics with Isothiocyanates: Evidence Supporting a Four-Step Domino Process and Ruling Out a [2 + 2] Mechanism

David Cantillo,<sup>\*,†</sup> Martín Ávalos,<sup>†</sup> Reyes Babiano,<sup>†</sup> Pedro Cintas,<sup>†</sup> José L. Jiménez,<sup>†</sup> Mark E. Light,<sup>‡</sup> and Juan C. Palacios<sup>†</sup>

Departamento de Química Orgánica e Inorgánica, QUOREX Research Group, Facultad de Ciencias, Universidad de Extremadura, E-06071 Badajoz, Spain, and Department of Chemistry, University of Southampton, Highfield, Southampton SO17 1BJ, U.K.

dcannie@unex.es

Received January 9, 2009



Mesoionic heterocycles derived from 1,3-thiazolium-4-olates (thioisomünchnones) undergo thionation with aryl isothiocyanates to afford the corresponding 4-thiolate derivatives. Here, we document this transformation in detail, giving a crystallographic characterization of the solid-state structures. From the mechanistic viewpoint, the formal thionation process could be consistent with a [2 + 2] reaction of the exocyclic C–O bond of the thioisomünchnone with the C=S double bond of the isothiocyanate moiety, which would be competing with a (3 + 2) process as usual in mesoionic rings. Theoretical computations at the [B3LYP/6-31G(d):PM3] level, in which only bond-forming and bond-breaking reactions and neighboring atoms are treated at the DFT level, do reproduce the experimental results and rule out the expected pathway. Calculations instead suggest the existence of a four-step domino pathway through several polar intermediates that agrees with the electronic nature of the substituents involved. The mechanistic hypothesis has further been corroborated by an experiment with isotopically <sup>13</sup>C-labeled PhNCS that unambiguously shows the way in which the exchange reaction occurs.

### Introduction

The possibility of rationalizing chemical reactions, which are formally cycloadditions, as nonconcerted processes, represents a challenging domain of theoretical chemistry. A suitable scenario in this pursuit is provided by mesoionic heterocycles, which contain a masked allyl-type 1,3-dipole and are able to react with a variety of dipolarophiles giving rise to synthetically useful functionalized heterocycles.<sup>1</sup> Mesoionics do usually react via concerted asynchronous pathways, although in some cases, both theory and experiment point to a stepwise transformation. Among mesoionic rings, 1,3-thiazolium-4-olates (colloquially referred to as thioisomünchnones) have proven to be versatile synthons leading to a variety of heterocycles hitherto unknown in 1,3-dipolar cycloadditions.<sup>2</sup>

Mesoionic heterocycles decorated with an exocyclic sulfur atom (i.e., thiolates) have recently gained attention due to their greater stability and potential behavior as photonic materials with NLO properties.<sup>3</sup> Chasing this structural goal, we have recently reported the transformation of a chiral imidazo[2,1-*b*]thiazolium-3-olate (**1**) into imidazo[2,1-*b*]thiazolium-3-thiolate (**2**) and 4-thioxoimidazo[1,2-*a*]pyrimidinium-6-olate (**3**) systems by reaction with aryl isothiocyanates (Ar<sup>2</sup>NCS).<sup>4</sup> In these processes, variable amounts of 4-oxoimidazo[1,2-*a*]pyrimidinium-6-olates (**4**) were also isolated.

The kinetic and thermodynamic stability of **2**, which can be stored for long periods without apparent decomposition and does

(3) (a) Bosco, C. A. C.; Maciel, G. S.; Rakov, N.; de Araújo, C. B.; Acioli, L. H.; Simas, A. M.; Athayde-Filho, P. F.; Miller, J. *Chem. Phys. Lett.* **2007**, *449*, 101–106. (b) Pilla, V.; de Araújo, C. B.; Lira, B. F.; Simas, A. M.; Miller, J.; Athayde-Filho, P. F. *Opt. Commun.* **2006**, *264*, 225–228. (c) Menezes, L. de S.; de Araújo, C. B.; Alencar, M. A. R. C.; Athayde-Filho, P. F.; Miller, J.; Simas, A. M. *Chem. Phys. Lett.* **2001**, *347*, 163–66. (d) Rakov, N.; de Araújo, C. B.; da Rocha, G. B.; Simas, A. M.; Athayde-Filho, P. F.; Miller, J. *Chem. Phys. Lett.* **2000**, *332*, 13–18. (e) Bezerra, A. G., Jr.; Gomes, A. S. L.; Athayde-Filho, P. F.; da Rocha, G. B.; Miller, J.; Simas, A. M. *Chem. Phys. Lett.* **1999**, *309*, 421–426.

(4) Cantillo, D.; Ávalos, M.; Babiano, R.; Cintas, P.; Jiménez, J. L.; Light, M. E.; Palacios, J. C. *Org. Lett.* **2008**, *10*, 1079–1082.

<sup>†</sup> Universidad de Extremadura.

<sup>‡</sup> University of Southampton.

(1) Gribble, G. W. In *Synthetic Applications of 1,3-Dipolar Cycloaddition Chemistry toward Heterocycles and Natural Products*; Padwa, A., Pearson, W. H., Eds.; Wiley: New York, 2003; pp 681–753.

(2) Ávalos, M.; Babiano, R.; Cintas, P.; Jiménez, J. L.; Palacios, J. C. *Acc. Chem. Res.* **2005**, *38*, 460–468.

## CHART 1

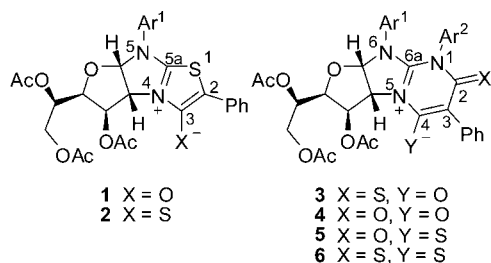
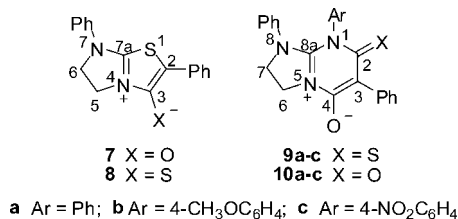


## CHART 2



not react with aryl iso(thio)cyanates under the same conditions described for **1**, equally explains why the alternative 4-oxoimidazo[1,2-*a*]pyrimidinium-6-thiolate (**5**) or 4-thioimidazo[1,2-*a*]pyrimidinium-6-thiolate (**6**) systems have never been detected (Chart 1).

The present paper documents in detail this conceptually simple oxygen–sulfur exchange, giving further structural insights into the nature of the polycyclic system attained and providing a rationale consistent with a stepwise mechanism. That the heterocumulenic isothiocyanate reacts through a [2 + 2] pathway as the logical surrogate has also been disproved.

## Results and Discussion

**Syntheses and Structure.** The reaction of **1** with aryl isothiocyanates exhibits a general pattern. Thus, reactions of the imidazo[2,1-*b*]thiazolium-3-olate **7**<sup>5,6</sup> with phenyl-, 4-methoxyphenyl-, and 4-nitrophenyl isothiocyanate afford the imidazo[2,1-*b*]thiazolium-3-thiolate **8** with variable amounts of the corresponding 4-thioimidazo[1,2-*a*]pyrimidinium-6-olate (**9a–c**) and 4-oxoimidazo[1,2-*a*]pyrimidinium-6-olate (**10a–c**) systems (Chart 2).

Compounds **10a–c** were isolated in low yields, although they could also be synthesized by direct reaction of **7** with phenyl-, 4-methoxyphenyl-, and 4-nitrophenyl isocyanate, respectively, in CH<sub>2</sub>Cl<sub>2</sub> at room temperature.

Gratifyingly, suitable crystals for X-ray diffraction could be obtained in the case of compounds **8**, **9b**, and **10a**, thus solving their structures unequivocally (Figure 1). Crystallographic data for compounds **8**, **9b**, and **10a** reveal that the formation of the crystalline lattice is governed by aryl ring interactions, which adopt favorable edge-to-face or offset stacked arrangements. The stacking shape depends on dipole–dipole interactions, a structural motif that can be easily visualized<sup>7</sup> (see Supporting Information).

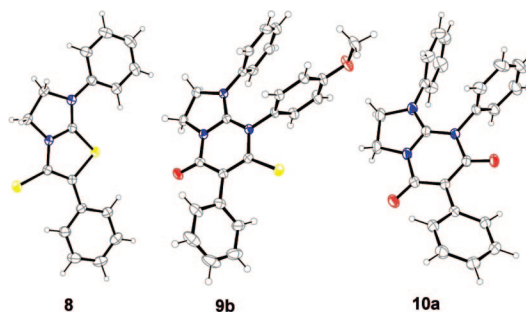


FIGURE 1. Molecular structures of **8**, **9b**, and **10a** as emerged from X-ray diffraction analyses.

<sup>1</sup>H NMR spectra of compounds **7–10** are extremely simple, although they show striking differences that facilitate their interpretation. Thus, the signals of the ethylene fragments appear as two well-defined triplets in the spectra of **9a–c**, whereas they adopt the shape of a pair of triple doublets for **7** and **10a–c** and resonate as a complex multiplet in the case of **8**. Moreover, distinction between structures **7**, **8** and **9**, **10** can be easily obtained by integration of their aromatic proton signals. <sup>13</sup>C NMR spectra of **7–10** also exhibit diagnostic differences. Thiocarbonylic carbons (C-2) of **9a–c** resonate at ~178 ppm, whereas the corresponding carbonylic carbons of **10a–c** appear at ~160 ppm, and in both cases, the carbons (C-3) more affected by the negative charge delocalization are strongly shielded ( $\delta$  ~114 and ~88 ppm for **9a–c** and **10a–c**, respectively). By invoking the same argument, the signals of the C-2 carbon atoms in thioisomünchnones **7** and **8** are also shifted upfield (81.6 and 111.6 ppm, respectively).

At first glance, the transformation of thioisomünchnones **1** and **7** into their thio derivatives **2** and **8**, which has no antecedents in the literature, could be interpreted as an O/S exchange resulting from a stepwise [2 + 2] cycloaddition reaction of the C–O<sup>−</sup> bond of **1** and **7** with the thiocarbonyl group of the aryl isothiocyanate, in an analogous fashion to the dimerization of some isothiocyanates.<sup>8</sup> This [2 + 2] cycloaddition could compete with the concerted (3 + 2) cycloadditions of the thiocarbonyl ylide, masked in **1** and **7**, with the C=N double bonds of the aryl isothiocyanate and the aryl isocyanate generated during the formation of **2** and **8**. In such processes, betaines **3**, **4**, **9**, and **10** could be formed by sulfur extrusion from the nonisolated initial cycloadducts (Scheme 1).

In order to prove this hypothesis and since theoretical modeling of the whole polycyclic chiral system would require an enormous computational cost at an ab initio level, we have carried out a computational study on the reactivity of **1** (Ar<sup>1</sup> = Ph) with phenyl isothiocyanate using the ONIOM[B3LYP/6-31G(d):PM3]<sup>9,10</sup> method. Taking into account the chiral nature of **1**, we have considered in each case two reaction channels to simulate the approaches of phenyl isothiocyanate to both faces of the mesoionic ring of **1**. Figure 2 depicts these approaches (*endo* and *exo*) for the optimized structures of both reagents, in which balls and sticks represent the partial system treated at the B3LYP/6-31G(d) level while the wire-shaped structure

(5) Arecas, P.; Ávalos, M.; Babiano, R.; González, L.; Jiménez, J. L.; Méndez, M. M.; Palacios, J. C. *Tetrahedron Lett.* **1993**, *34*, 2999–3002.

(6) Ávalos, M.; Babiano, R.; Cintas, P.; Hursthouse, M. B.; Jiménez, J. L.; Light, M. E.; López, I.; Palacios, J. C.; Silvero, G. *Chem.—Eur. J.* **2001**, *7*, 3033–3042.

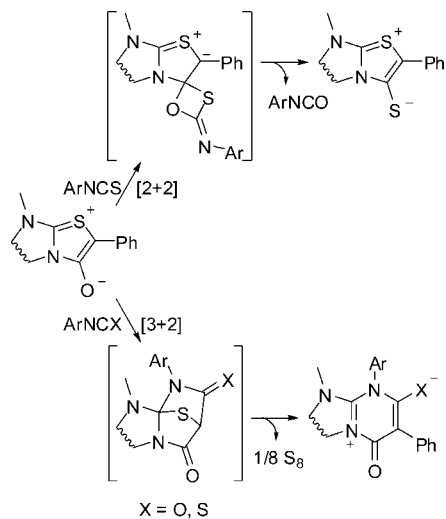
(7) Hunter, C. A.; Lawson, K. R.; Perkins, J.; Urch, C. J. *J. Chem. Soc., Perkin Trans. 2* **2001**, 651–669.

(8) (a) Adams, R. D.; Huang, M. *Eur. J. Org. Chem.* **1998**, 1025–1028. (b) Dickore, K.; Kuhle, E. *Angew. Chem., Int. Ed. Engl.* **1965**, *4*, 430.

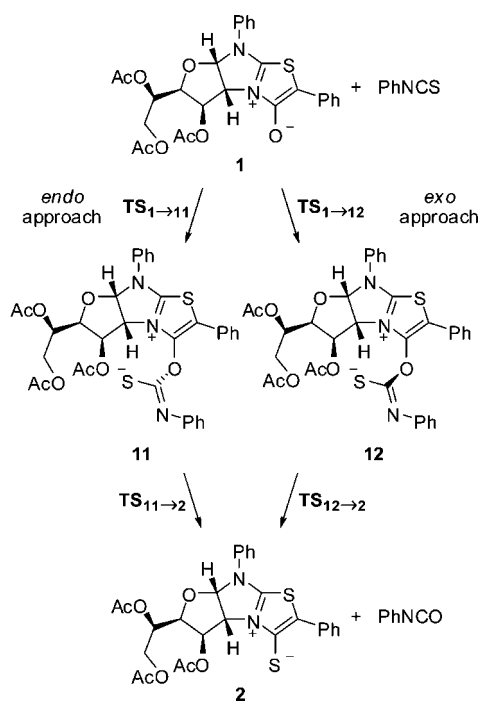
(9) Maseras, F.; Morokuma, K. *J. Comput. Chem.* **1995**, *16*, 1170–1179.

(10) Froese, R. D. J.; Morokuma, K. In *The Encyclopedia of Computational Chemistry*; Schleyer, P. v. R., Allinger, N. L., Clark, T., Gasteiger, J., Kollman, P. A., Schaefer, H. F., III, Schreiner, P. R., Eds.; John Wiley: Chichester, UK, 1998; pp 1245–1257.

## SCHEME 1



## SCHEME 2



corresponds to the molecular fragment assessed at a semiempirical level (PM3).

**endo and exo [2 + 2] Cycloadditions.** An analysis of the *endo* and *exo* [2 + 2] cycloadditions of the C=S double bond of phenyl isothiocyanate with the C–O<sup>−</sup> pseudodouble bond of **1** led to the location of the first transition structures (TS<sub>1-11</sub> and TS<sub>1-12</sub>) corresponding to the nucleophilic attack of the oxygen atom to the thiocarbonylic carbon. In both cases, these transition structures are stabilized by interactions of the sulfur atom with the hydrogens linked to the C-3' (*endo* approach) and C-2' (*exo* approach) carbon atoms of the sugar framework (S–H<sub>3</sub>: 1.864 Å for TS<sub>1-11</sub> and S–H<sub>2</sub>: 1.811 Å for TS<sub>1-12</sub>). Transition structures (TS<sub>1-11</sub> and TS<sub>1-12</sub>) evolved into two zwitterionic intermediates (**11** and **12**), which in the rate-determining steps of both processes led to two new transition structures (TS<sub>11-2</sub> and TS<sub>12-2</sub>) corresponding to two internal concerted nucleophilic substitutions involving formation of C–S bonds and rupture of C–O bonds. These transformations

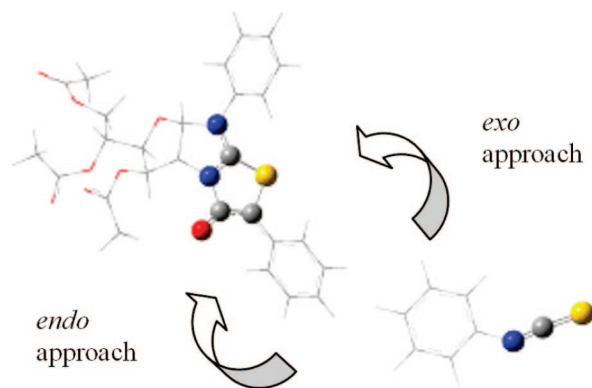


FIGURE 2. Approaches (*endo* and *exo*) of phenyl isothiocyanate to thioisomünchnone **1** (Ar<sup>1</sup> = Ph).

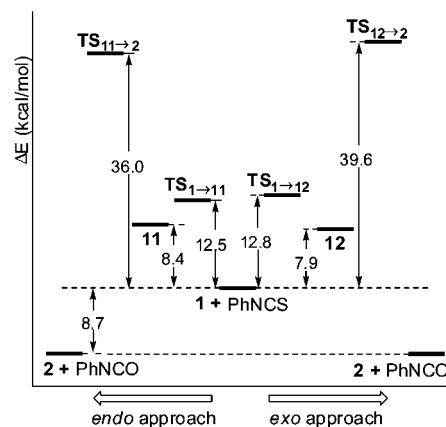


FIGURE 3. Energy profile for *endo* and *exo* [2 + 2] cycloadditions of **1** with PhNCS.

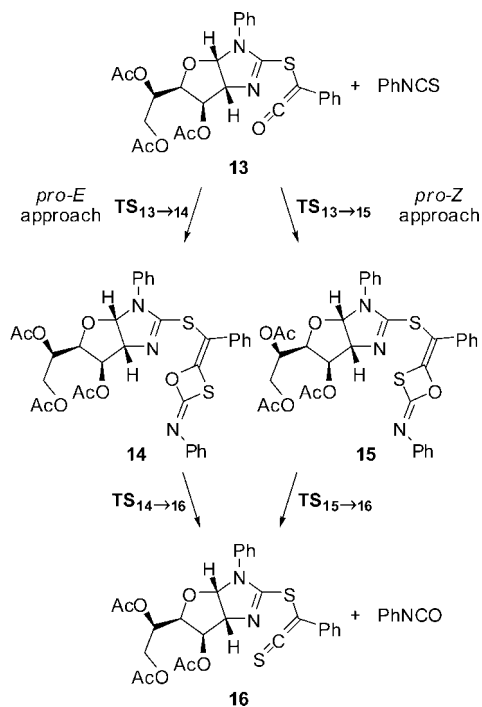
conclude with the release of phenyl isocyanate and formation of the imidazo[2,1-*b*]thiazolium-4-thiolate **2** (Scheme 2 and Figure 3).

Although we have not yet been able to demonstrate the existence of an equilibrium between thioisomünchnone **1** and its valence tautomer **13**, their relative electronic energies ( $\Delta E = 5.1$  kcal/mol) and the low energy of the transition structure corresponding to their mutual conversion ( $\Delta E = 8.1$  kcal/mol) suggest that the ketene intermediate **13** could also be involved in the transformation of **1** into **2**, which would likewise occur through two different approaches of the reactants. The free rotation of sulfur single bonds in compound **13** together with the coplanar disposition of phenyl isothiocyanate to the ketene during its approach to the carbon–oxygen double bond of the latter impedes use of the terms *endolexo* without ambiguity. In this particular situation, the stereochemical outcome has been defined in terms of prostereoisomerism descriptors relative to the *E/Z* configuration of the carbon–carbon double bond of the initial cycloadduct (Scheme 3).

Thus, for both approaches (*pro-E* and *pro-Z*), we have located the transition structures (TS<sub>13-14</sub> and TS<sub>13-15</sub>) that lead to the intermediate cycloadducts (**14** and **15**) and those coming from them (TS<sub>14-16</sub> and TS<sub>15-16</sub>) during their respective transformations into the valence tautomer (**16**) of **2**.

Data collected in Figure 4 show a similar energetics for both [2 + 2] cycloadditions (*pro-E* and *pro-Z*). As a result, the two approaches would take place with comparable rates had the ketenic valence tautomers been actually involved in the O/S exchange. However, the energy barriers of these processes are

SCHEME 3



~5 kcal/mol higher than the energy barrier corresponding to the slowest step of the *endo* [2 + 2] cycloaddition of the same mesoionic system (Figure 3). This fact, along with the greater stability of the mesoionic tautomer, suggests that the transformation of imidazo[2,1-*b*]thiazolium-3-olate systems into the corresponding imidazo[2,1-*b*]thiazolium-3-thiolates through [2 + 2] cycloaddition reactions would most likely involve the participation of the mesoionic tautomer.

**endo and exo (3 + 2) Cycloadditions.** Again, two reaction channels regarding the orientation of the dipolarophile with respect to the sugar framework (*endo* and *exo* approaches) should be established to define the 1,3-dipolar cycloaddition of **1** with phenyl isothiocyanate (Figure 2). Assuming that these cycloadditions follow a concerted mechanism, the first protocol was to locate the transition structures from the optimized geometries of cycloadducts **19a** and **20a**. However, we could not find one but two transition structures for either approach

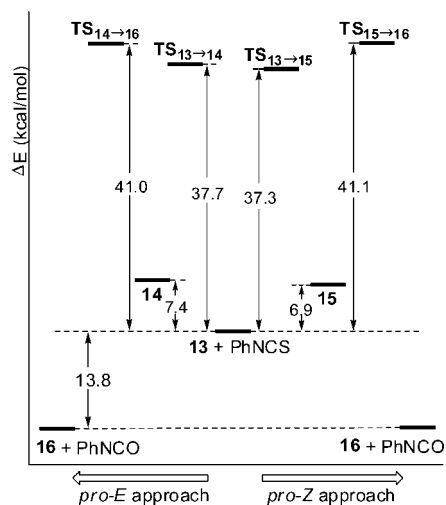
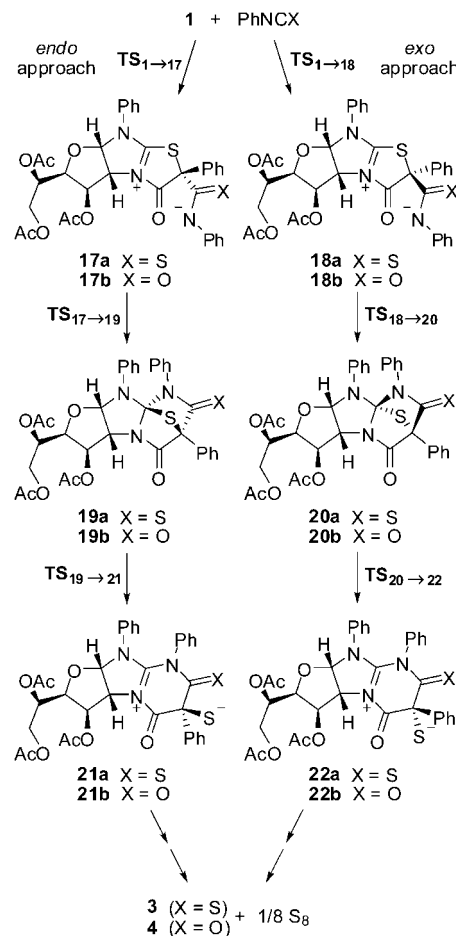


**FIGURE 4.** Energetics of an alternative pathway involving attacks of PhNCS to the ketene tautomer **13**.

SCHEME 4



(**TS**<sub>1→17a</sub>, **TS**<sub>17a→19a</sub> and **TS**<sub>1→18a</sub>, **TS**<sub>18a→20a</sub>). The transition structures **TS**<sub>1→17a</sub> and **TS**<sub>1→18a</sub> involve carbon–carbon bond formation, whereas structures **TS**<sub>17a→19a</sub> and **TS**<sub>18a→20a</sub> are concerned with the subsequent carbon–nitrogen bond-forming reactions. In addition, the corresponding zwitterionic intermediates (**17a** and **18a**) were optimized.

A stepwise sulfur extrusion from both **19a** and **20a** completes the betaine formation. Probably, the first step involves the C<sub>7</sub>–S bond breaking, a pathway favored by delocalization of a positive charge into the three neighboring nitrogen atoms of **21a** and **22a** (Scheme 4 and Figure 5).

For the transition structures **TS**<sub>19a→21a</sub> and **TS**<sub>20a→22a</sub>, corresponding to the ring opening of cycloadducts **19a** and **20a**, the C<sub>6a</sub>–S bond lengths are estimated to be 2.724 and 2.610 Å, respectively. The low energy barriers [ $E(\text{TS}_{19a→21a}) - E(\mathbf{19a}) = 8.5$  kcal/mol and  $E(\text{TS}_{20a→22a}) - E(\mathbf{20a}) = 9.8$  kcal/mol] are consistent with a spontaneous sulfur extrusion as observed experimentally.

All the above-described [2 + 2] cycloadditions, no matter the type of substrate that may participate (either the mesoionic system **1** or its valence tautomer **13**), involve the elimination of 1 equiv of phenyl isocyanate, which can further react with the remaining thioisomünchnone **1** to give rise to 4-oxoimidazo[1,2-*a*]pyrimidinium-6-olate **4**.

Again, the theoretical study allowed us to locate two transition structures (**TS**<sub>1→17b</sub>, **TS**<sub>17b→19b</sub>) and one zwitterionic intermediate (**17b**) for the *endo* approach, as well as for the *exo* counterpart (**TS**<sub>1→18b</sub>, **TS**<sub>18b→20b</sub>, and **18b**) leading to the corresponding

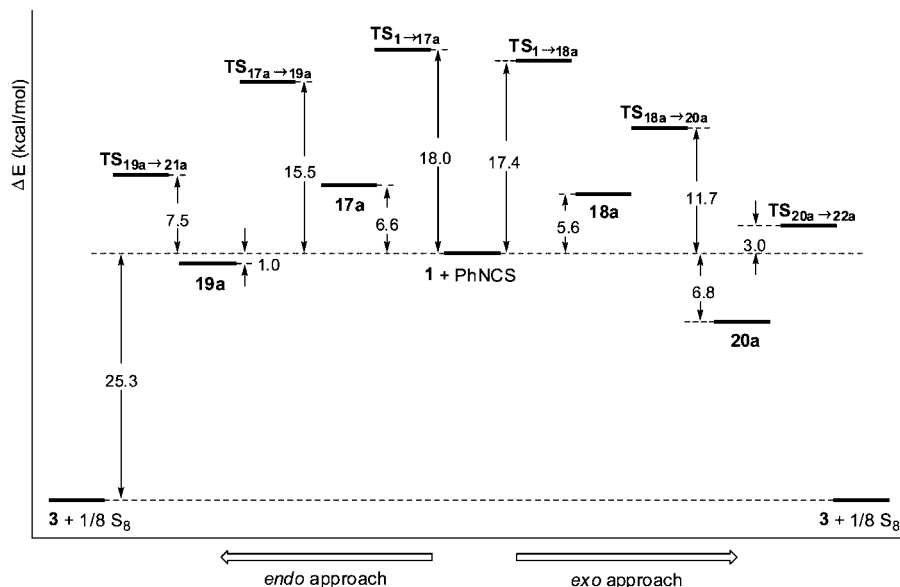


FIGURE 5. Reaction profiles for *endo* and *exo* approaches of PhNCS to **1** during a (3 + 2) cycloaddition.

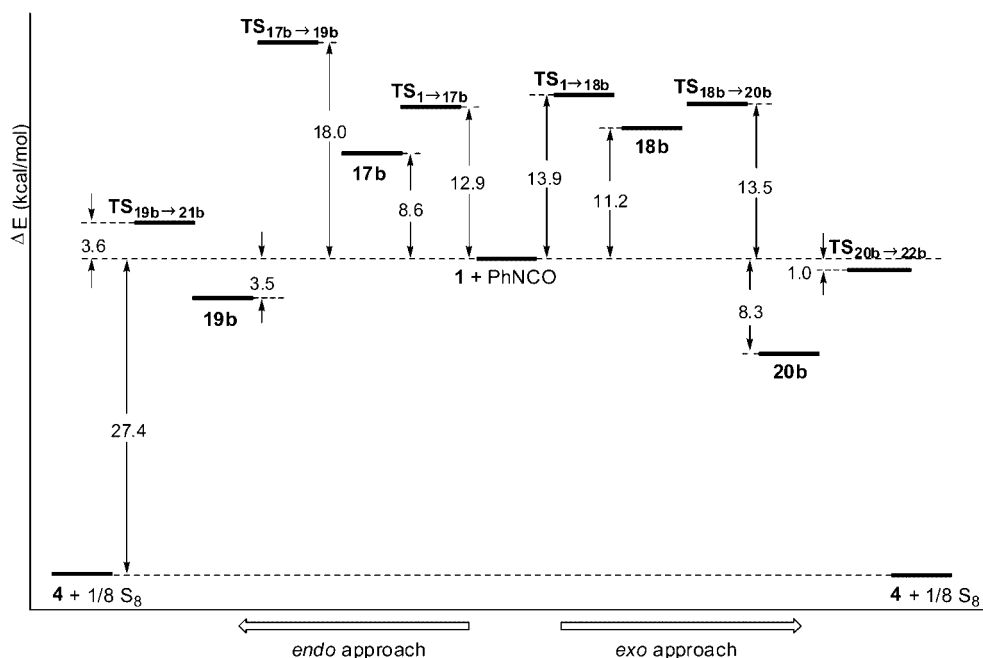


FIGURE 6. Energy profiles for *endo* and *exo* (3 + 2) cycloadditions of **1** and PhNCO.

cycloadducts **19b** and **20b**, respectively (Scheme 4). Their relative energies have been collected in Figure 6.

The energy barrier of the rate-determining step for the formation of betaine **3** (17.4 kcal/mol, see Figure 5) is considerably lower than any other energy barrier corresponding to the O/S exchange rationalized in terms of a [2 + 2] cycloaddition of phenyl isothiocyanate with thioisomünchnone **1** (36.0 kcal/mol, see Figure 3) or its valence tautomer **13** (41.0 kcal/mol, see Figure 4). Accordingly, the results exposed so far do not account for the formation of imidazo[2,1-*b*]thiazolium-3-thiolates (**2**) by reaction of **1** with aryl isothiocyanates nor do they satisfactorily explain the prevalence of such derivatives in many cases.<sup>4</sup>

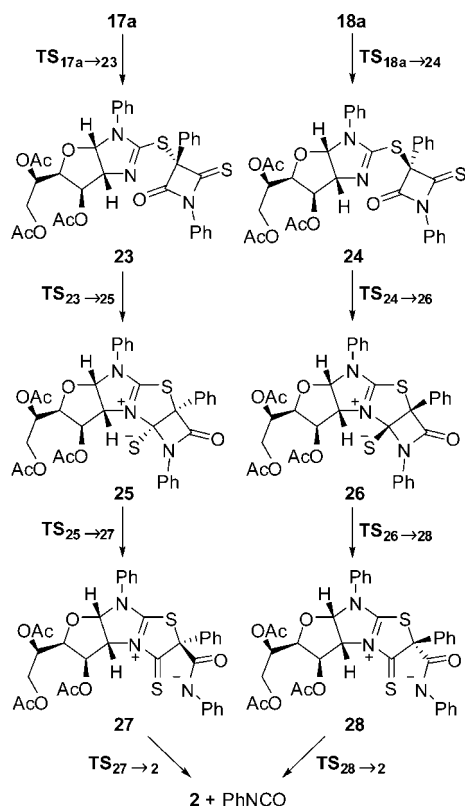
On the basis of these premises, we conjectured that the O/S reaction exchange undergone by imidazo[2,1-*b*]thiazolium-3-olate systems (**1** or **7**) might have taken place by a pathway other than the [2 + 2] cycloaddition described above.

#### Thionation of Imidazo[2,1-*b*]thiazolium-3-olates: An Alternative Mechanism.

The transformation of the 1,3-thiazolium-4-olate **1** into betaine **3** clearly shows its reactivity as thiocarbonyl ylide toward the nitrogen-carbon double bond of an aryl isothiocyanate. However, the theoretical calculations rule out a concerted mechanism for this 1,3-dipolar cycloaddition; rather, this reaction proceeds via a nonconcerted pathway that involves an open dipolar intermediate (**17a** or **18a**). Scheme 4 shows how the nucleophilic nitrogens of the intermediates **17a** and **18a**, arising from the attack of the C-2 atom of **1** to the thiocarbonyl carbon of phenyl isothiocyanate, would ultimately become linked to the C-5 atom of the original mesoionic, thus affording the cycloadducts **19a** and **20a** as precursors of betaine **3**. These nucleophilic nitrogens could also attack a vicinal carbonyl group (C-3 of **1**) leading to azetidines **23** and **24** by an intramolecular N-acylation. This process could also be favored by the good leaving group character of the thioami-



SCHEME 5



dinium framework. The free rotation around the C–S bonds of **23** and **24** would likewise enable the intramolecular nitrogen attack onto the azetidinic thiocarbonyl group leading to two new dipolar intermediates (**27** and **28**) and, finally, to **2** after elimination of the corresponding aryl isocyanate fragment (Scheme 5).

This mechanistic hypothesis has also been theoretically investigated by means of the ONIOM[B3LYP/6-31G(d):PM3] method, taking newly into account the two possible trajectories of reactants (*endo* and *exo*). The zwitterionic intermediates **17a** and **18a** evolve into the azetidines **23** and **24** through a first transition structure (TS<sub>17a→23</sub> and TS<sub>18a→24</sub>). The intramolecular nucleophilic attack to the thiocarbonyl group of **23** and **24** involves the formation of a first transition structure (TS<sub>23→25</sub> and TS<sub>24→26</sub>), a tetrahedral intermediate (**25** and **26**), as well as a new transition structure (TS<sub>25→27</sub> and TS<sub>26→28</sub>) leading to a dipolar intermediate (**27** and **28**), which then loses aryl isocyanate to give the 1,3-thiazolium-4-thiolate **2** via the transition structures TS<sub>27→2</sub> and TS<sub>28→2</sub>. Figure 7 compiles the relative electronic energies for the full-optimized structures.

On the basis of the relative electronic energies for the structures depicted in Figures 5–7, one can plausibly interpret the experimental results found in the reactions of the imidazo[2,1-*b*]thiazolium-3-olates **1** with aryl isothiocyanates. Although the *exo* approach of aryl isothiocyanate is slightly favored, the similar stability of structures TS<sub>1→17a</sub> and TS<sub>1→18a</sub> ( $\Delta E = 0.6$  kcal/mol) requires an assessment of both reaction pathways, which would lead to the zwitterionic intermediates **17a** and **18a** ( $\Delta E = 1.0$  kcal/mol). Such dipolar species could now evolve into cycloadducts **19a** and **20a** ( $\Delta E = 5.8$  kcal/mol) by the anionic nitrogen attack to the C-5a carbon atom of **1**, thus overcoming energy barriers of 8.9 and 6.1 kcal/mol, respectively. Moreover, they could evolve into azetidines **23**

and **24** ( $\Delta E = 1.1$  kcal/mol) by attack of the same nitrogen atom to the C-3 atom, overcoming in this case energy barriers of only 2.2 and 5.1 kcal/mol. These low values would also justify the formation of **23** and **24** as major products at the expense of cycloadducts **19a** and **20a**. The optimal disposition of the imidazoline nitrogen of **23** and **24** facilitates its intramolecular nucleophilic attack onto the thiocarbonyl group of the azetidene ring, which would lead to two new dipolar intermediates (**27** and **28**) and, finally, to the imidazo[2,1-*b*]thiazolium-3-thiolate **2**.

The preceding analyses reveal two further keypoints as well. First, a comparison of Figures 5 and 6 reveals the greater reactivity between **1** and phenyl isocyanate than the combination of **1** and phenyl isothiocyanate. Second, a similar inspection of the electronic energy differences (Figure 7) accounts for the low reactivity of **2** against phenyl isocyanate, a process unlikely to occur, thereby validating the experimental results still further.

**In Search of a Nonconcerted Pathway: A Further Experimental Assessment.** Unlike the expected O/S exchange reaction resulting from a [2 + 2] cycloaddition (Scheme 1), the proposed mechanism outlined in Scheme 4 involves the C–O bond substitution in compound **1** by a new C–S bond coming from the isothiocyanate partner. Although the above computational study supports this surmise, we sought a further experimental verification to reinforce the mechanistic picture. Having this goal in mind, the mesoionic derivative **1** (Ar<sup>1</sup> = Ph) was reacted with isotopically labeled PhN<sup>13</sup>CS and the process monitored by <sup>13</sup>C NMR spectroscopy.<sup>11</sup> Figure 8 shows the <sup>13</sup>C NMR spectrum of the imidazo[2,1-*b*]thiazolium-3-thiolate system obtained in this transformation, in which one can appreciate both the strong enhancement in intensity for the pseudothiocarbonyl carbon signal (C-3,  $\delta$  148.7 ppm) and the splitting of the C-2 signal, which appears at 110.6 ppm ( $J_{C2,C3} = 77.2$  Hz). Moreover, the  $\beta$  carbon atoms relative to C-3 (i.e., C-5a and the phenyl carbon atom linked to C-2) resonate as doublets:  $\delta$  159.7 ppm ( $J = 5.2$  Hz) and  $\delta$  133.2 ppm ( $J = 3.8$  Hz), respectively. This observation clearly supports the exchange reaction of the C–O bond by the <sup>13</sup>C–S bond during the thionation of thioisomünchnones with aryl isothiocyanates.

## Concluding Remarks

The present work provides an in-depth structural, experimental, and theoretical study for the thionation of 1,3-thiazolium-4-olates with aryl isothiocyanates leading to the most promising and stable thiolate systems. From a mechanistic viewpoint, this transformation is consistent with a four-step domino reaction that lacks precedents in the literature. This aspect is supported by data obtained through the reaction with <sup>13</sup>C-labeled phenyl isothiocyanate, thus unequivocally demonstrating the substitution of the C–O bond by the <sup>13</sup>C–S bond at the mesoionic ring. Furthermore, an ONIOM-based theoretical methodology has been performed to simulate the complex chemical reaction at a relatively low computational cost, in which only the heavy atoms involved in bond-forming and bond-breaking processes and their immediate (or first sphere) neighbors are computed at the B3LYP/6-31G(d) level. It is worth noting that this methodology detects the existence of zwitterionic intermediates accounting for the range of subsequent products observed experimentally. In addition, theory discards

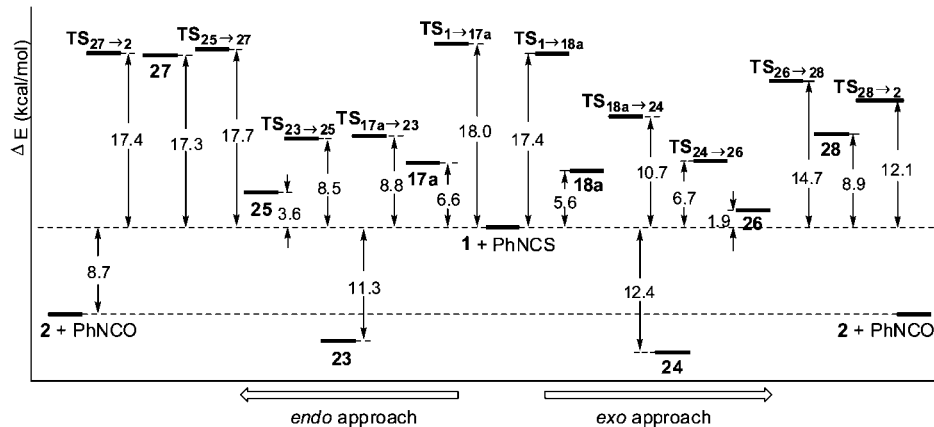


FIGURE 7. Energetics of the domino sequence involving the thionation of **1** with PhNCS.

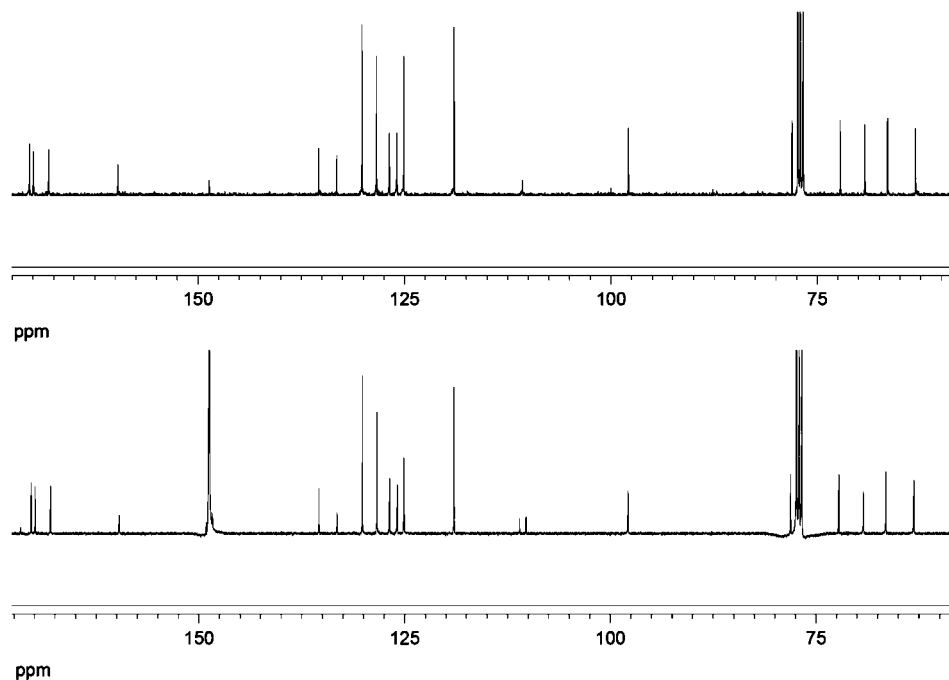


FIGURE 8.  $^{13}\text{C}$  NMR spectra of the chiral imidazo[2,1-*b*]thiazolium-3-thiolate **2** obtained from thioisomünchnone **1** and PhNCS (top) and PhN $^{13}\text{C}$ S (bottom), respectively.

an alternative and more logical [2 + 2] cycloaddition with the heterocumulenic partner.<sup>12</sup>

## Experimental Section

**General Procedure for the Reaction of Thioisomünchnone **7** with Aryl Isothiocyanates:** To a suspension of **7** (3 mmol) in dichloromethane (30 mL) was added the corresponding aryl isothiocyanate (15 mmol). The reaction mixture was stirred at room temperature and monitored by TLC (benzene/acetonitrile 3:1) until the complete disappearance of **7** (no more than 24 h). Then, it was evaporated, and the resulting crude mixture was purified by flash chromatography (benzene/acetonitrile gradient elution from 5:1 to 1:5).

(11) Ares, J. J.; Fowble, J. W.; Urchek, T. G.; Miller, D. D. *Biochem. Biophys. Res. Commun.* **1987**, *142*, 1064–1071.

(12) One of the reviewers has suggested to compute the corresponding transition structures for the rate-determining step of both domino and [2 + 2] reactions of compound **7** and PhNCS at a pure B3LYP/6-31G(d) level and using the IRC method. In doing so, we were able to obtain a significant energy difference between such TSs (21.8 kcal/mol), thereby fully corroborating the mechanistic proposal and supporting the ONIOM[B3LYP/6-31G(d);PM3] method as a reliable approach (see Supporting Information).

**Reaction of **7** with Phenyl Isothiocyanate.** Following the above general procedure, the condensation of **7** and phenyl isothiocyanate gave rise to **8** (73%), **9a** (10%), and **10a** (4%).

**2,7-Diphenyl-5*H*,6*H*,7*H*-imidazo[2,1-*b*]-1,4-thiazolium-3-thiolate (**8**):** mp 264–265 °C;  $^1\text{H}$  NMR (400 MHz,  $\text{CDCl}_3$ )  $\delta$  8.19 (d, 2H,  $J = 7.2$  Hz, Ar), 7.48 (t, 2H,  $J = 7.6$  Hz, Ar), 7.31 (t, 2H,  $J = 7.6$  Hz, Ar), 7.25 (t, 1H,  $J = 7.6$  Hz, Ar), 7.15 (t, 1H,  $J = 7.2$  Hz, Ar), 7.14 (d, 2H,  $J = 8.0$  Hz, Ar), 4.67 (m, 4H, 2CH<sub>2</sub>);  $^{13}\text{C}$  NMR (100 MHz,  $\text{CDCl}_3$ )  $\delta$  158.4, 148.3, 137.0, 133.5, 130.2, 128.4, 125.9, 125.4, 125.2, 116.3, 111.6, 52.0, 45.6. Anal. Calcd for C<sub>17</sub>H<sub>14</sub>N<sub>2</sub>S<sub>2</sub>: C, 65.77; H, 4.55; N, 9.02; S, 20.66. Found: C, 65.52; H, 4.76; N, 8.93; S, 20.45.

**1,3,8-Triphenyl-4-oxoimidazo[1,2-*a*]pyrimidin-5-ylidium-2-thiolate (**9a**):** mp 267–268 °C;  $^1\text{H}$  NMR (400 MHz,  $\text{CDCl}_3$ )  $\delta$  7.52 (d, 2H,  $J = 7.8$  Hz, Ar), 7.37 (t, 2H,  $J = 7.6$  Hz, Ar), 7.24 (t, 1H,  $J = 7.6$  Hz, Ar), 7.11 (m, 3H, Ar), 6.97 (m, 5H, Ar), 6.79 (d, 2H,  $J = 8.0$  Hz, Ar), 4.41 (t, 2H,  $J = 9.4$  Hz, CH<sub>2</sub>), 4.06 (t, 2H,  $J = 9.4$  Hz, CH<sub>2</sub>);  $^{13}\text{C}$  NMR (100 MHz,  $\text{CDCl}_3$ )  $\delta$  177.9, 154.8, 150.7, 137.6, 137.4, 136.1, 131.3, 130.6, 129.7, 129.2, 128.8, 128.4, 128.0, 127.6, 126.7, 114.8, 53.8, 41.9. Anal. Calcd for C<sub>24</sub>H<sub>19</sub>N<sub>3</sub>OS: C, 75.52; H, 4.82; N, 10.57; S, 8.07. Found: C, 75.27; H, 4.87; N, 10.72; S, 7.86.

**1,3,8-Triphenyl-4-oxoimidazo[1,2-*a*]pyrimidin-5-ylum-2-olate (10a):** mp 378–380 °C; <sup>1</sup>H NMR (400 MHz, DMSO-*d*<sub>6</sub>) δ 7.66 (d, 2H, *J* = 8.0 Hz, Ar), 7.19 (t, 2H, *J* = 7.6 Hz, Ar), 7.03 (m, 11H, Ar), 4.20 (t, 2H, *J* = 8.8 Hz, CH<sub>2</sub>), 4.11 (t, 2H, *J* = 8.4 Hz, CH<sub>2</sub>); <sup>13</sup>C NMR (100 MHz, DMSO-*d*<sub>6</sub>) δ 160.1, 158.7, 149.6, 138.0, 137.0, 133.9, 130.6, 130.5, 129.2, 128.7, 128.5, 128.2, 127.8, 127.2, 124.2, 88.8, 53.1, 42.2. Anal. Calcd for C<sub>24</sub>H<sub>19</sub>N<sub>3</sub>O<sub>2</sub>: C, 75.57; H, 5.02; N, 11.02. Found: C, 75.63; H, 5.27; N, 11.06.

**Reaction of 7 with 4-Methoxyphenyl Isothiocyanate.** Following the general procedure, reaction of 7 and 4-methoxyphenyl isothiocyanate afforded **8** (9%), **9b** (34%), and **10b** (4%).

**3,8-Diphenyl-1-(4-methoxyphenyl)-4-oxoimidazo[1,2-*a*]pyrimidin-5-ylum-2-thiolate (9b):** mp 284–285 °C; <sup>1</sup>H NMR (400 MHz, CDCl<sub>3</sub>) δ 7.54 (d, 2H, *J* = 8.0 Hz, Ar), 7.36 (t, 2H, *J* = 7.6 Hz, Ar), 7.22 (t, 1H, *J* = 7.6 Hz, Ar), 7.10 (m, 3H, Ar), 6.82 (d, 2H, *J* = 8.8 Hz, Ar), 6.75 (d, 2H, *J* = 7.2 Hz, Ar), 6.44 (d, 2H, *J* = 8.8 Hz, Ar), 4.30 (t, 2H, *J* = 9.2 Hz, CH<sub>2</sub>), 3.92 (t, 2H, *J* = 9.4 Hz, CH<sub>2</sub>), 3.64 (s, 3H, OCH<sub>3</sub>); <sup>13</sup>C NMR (100 MHz, CDCl<sub>3</sub>) δ 178.1, 159.5, 155.0, 150.8, 137.8, 137.7, 131.7, 131.5, 129.5, 128.8, 128.4, 127.9, 127.7, 126.5, 114.4, 113.6, 55.3, 53.6, 41.9. Anal. Calcd for C<sub>25</sub>H<sub>21</sub>N<sub>3</sub>O<sub>2</sub>S: C, 70.24; H, 4.95; N, 9.83; S, 7.50. Found: C, 70.25; H, 5.11; N, 9.90; S, 7.41.

**3,8-Diphenyl-1-(4-methoxyphenyl)-4-oxoimidazo[1,2-*a*]pyrimidin-5-ylum-2-olate (10b):** mp 319–320 °C; <sup>1</sup>H NMR (400 MHz, DMSO-*d*<sub>6</sub>) δ 7.68 (dd, 2H, *J* = 1.2, 8.4 Hz, Ar), 7.19 (t, 2H, *J* = 7.6 Hz, Ar), 7.01 (t, 1H, *J* = 7.6 Hz, Ar), 6.95 (dd, 2H, *J* = 2.4, 6.8 Hz, Ar), 6.52 (dd, 2H, *J* = 2.0, 6.8 Hz, Ar), 4.19 (dt, 2H, *J* = 2.4, 10.4 Hz, CH<sub>2</sub>), 4.10 (dt, 2H, *J* = 2.4, 10.4 Hz, CH<sub>2</sub>); <sup>13</sup>C NMR (100 MHz, DMSO-*d*<sub>6</sub>) δ 160.3, 159.2, 158.6, 149.8, 138.1, 137.1, 131.5, 130.4, 129.1, 127.9, 127.9, 127.1, 126.4, 124.1, 113.7, 88.7, 55.8, 53.0, 42.2. Anal. Calcd for C<sub>25</sub>H<sub>21</sub>N<sub>3</sub>O<sub>3</sub>: C, 72.98; H, 5.14; N, 10.21. Found: C, 72.76; H, 5.03; N, 10.43.

**Reaction of 7 with 4-Nitrophenyl Isothiocyanate.** Following the general procedure, reaction of 7 and 4-nitrophenyl isothiocyanate gave rise to **8** (81%), **9c** (3%), and **10c** (5%).

**3,8-Diphenyl-1-(4-nitrophenyl)-4-oxoimidazo[1,2-*a*]pyrimidin-5-ylum-2-thiolate (9c):** mp 198–199 °C; <sup>1</sup>H NMR (400 MHz, CDCl<sub>3</sub>) δ 7.81 (d, 2H, *J* = 8.8 Hz, Ar), 7.50 (d, 3H, *J* = 7.2 Hz, Ar), 7.38 (t, 3H, *J* = 7.6 Hz, Ar), 7.16 (m, 4H, Ar), 6.86 (d, 2H, *J* = 7.6 Hz, Ar), 4.47 (t, 2H, *J* = 9.4 Hz, CH<sub>2</sub>), 4.16 (t, 2H, *J* = 9.4 Hz, CH<sub>2</sub>); <sup>13</sup>C NMR (100 MHz, CDCl<sub>3</sub>) δ 184.5, 155.7, 150.4, 147.4, 132.0, 131.2, 130.1, 129.5, 128.1, 127.8, 127.0, 123.4, 118.0, 114.1, 53.8, 42.1. Anal. Calcd for C<sub>24</sub>H<sub>18</sub>N<sub>4</sub>O<sub>3</sub>S: C, 65.14; H, 4.10; N, 12.66; S, 7.25. Found: C, 64.86; H, 4.27; N, 12.62; S, 7.12.

**3,8-Diphenyl-1-(4-nitrophenyl)-4-oxoimidazo[1,2-*a*]pyrimidin-5-ylum-2-olate (10c):** mp 350–351 °C; <sup>1</sup>H NMR (400 MHz, DMSO-*d*<sub>6</sub>) δ 7.85 (dd, 2H, *J* = 4.0, 6.8 Hz, Ar), 7.66 (d, 2H, *J* = 7.2 Hz, Ar), 7.42 (dd, 2H, *J* = 4.0, 6.8 Hz, Ar), 7.20 (t, 2H, *J* = 7.6 Hz, Ar), 7.07 (m, 6H, Ar), 4.21 (dt, 2H, *J* = 1.8, 6.8 Hz, CH<sub>2</sub>),

4.15 (dt, 2H, *J* = 2.0, 6.8 Hz, CH<sub>2</sub>); <sup>13</sup>C NMR (100 MHz, DMSO-*d*<sub>6</sub>) δ 159.7, 158.8, 149.3, 147.2, 140.1, 137.5, 136.6, 132.3, 130.6, 129.5, 128.6, 128.0, 127.4, 124.6, 123.6, 88.9, 52.9, 42.4. Anal. Calcd for C<sub>24</sub>H<sub>18</sub>N<sub>4</sub>O<sub>4</sub>: C, 67.60; H, 4.25; N, 13.14. Found: C, 67.28; H, 4.29; N, 13.19.

**General Procedure for the Reaction of 7 with Aryl Iso-cyanates:** To a suspension of 7 (3 mmol) in dichloromethane (30 mL) was added the corresponding aryl isocyanate (3 mmol). The reaction mixture was stirred at room temperature and monitored by TLC (benzene/acetonitrile 3:1) until the complete disappearance of 7 (no more than 24 h). Then, it was evaporated, and the resulting crude mixture was purified by flash chromatography (benzene/acetonitrile, gradient elution from 3:1 to 1:5).

**Reaction of 7 with Phenyl Isocyanate.** Following the general procedure from 7 and phenyl isocyanate, compound **10a** was obtained in 52% yield.

**Reaction of 7 with 4-Methoxyphenyl Isocyanate.** Following the general procedure, reaction of 7 with 4-methoxyphenyl isocyanate produced **10b** (52%).

**Reaction of 7 with 4-Nitrophenyl Isocyanate.** Following the general procedure, reaction of 7 and 4-nitrophenyl isocyanate gave **10c** (18%).

**Reaction of 2,5-Diphenyl-(3,5,6-tri-*O*-acetyl-1,2-dideoxy- $\alpha$ -D-glucofurano)[1',2':4,5]-4*aH*,4*bH*-imidazo[2,1-*b*]thiazolium-3-olate (1) with <sup>13</sup>C-Labeled Phenyl Isothiocyanate.** To a solution of 1 (1 mmol) in dichloromethane (20 mL) was added PhN<sup>13</sup>CS (1 mmol). The reaction mixture was kept at room temperature and monitored by TLC (benzene/acetonitrile 3:1) until observing the disappearance of 1 (no more than 48 h). Then, it was filtered off, evaporated, and the resulting crude mixture was purified by flash chromatography (benzene/acetonitrile, gradient elution from 10:1 to 1:3) to give <sup>13</sup>C-labeled **2** (Ar<sup>1</sup> = Ph) (19%) and **4** (Ar<sup>1</sup> = Ar<sup>2</sup> = Ph)<sup>4</sup> (17%).

**Acknowledgment.** This work was supported by the Ministerio de Educación y Ciencia and FEDER (CTQ2005-07676 and CTQ2007- 66641) and the Junta de Extremadura (PRI07A016 and PRI08A032). D.C. thanks the Spanish Ministerio de Educación y Ciencia for a fellowship.

**Supporting Information Available:** <sup>1</sup>H and <sup>13</sup>C NMR spectra for all new compounds, crystal data for compounds **8**, **9b**, and **10a** in CIF format, and computational data for all structures computed at the ONIOM[B3LYP/6-31G(d):PM3]. This material is available free of charge via the Internet at <http://pubs.acs.org>.

JO900028C